NOTE

Subepicardial burn injuries in bullfrog heart induce electrocardiogram changes mimicking inferior wall myocardial infarction

Itsuro KAZAMA[1)]*, Ryo KUWANA[1)], Mizuki MUTO[1)], Amu NAGANO[1)],
Ririka FUJIMURA[1)], Ayano ASADA[1)], Tsutomu TAMADA[2)], Makoto SHIMOYAMA[1)]

[1)]Miyagi University, School of Nursing, Miyagi, Japan
[2)]Department of Respiratory Medicine, Tohoku University Graduate School of Medicine, Miyagi, Japan

ABSTRACT. Using bullfrog hearts, we previously reproduced a ST segment elevation in electrocardiogram (ECG), mimicking human ischemic heart disease. In the present study, by inducing subepicardial burn injuries on the inferior part of the frog heart ventricle, we could reproduce typical ECG changes observed in human inferior wall myocardial infarction, such as the marked elevation of the ST segments in inferior limb leads (II, III, aVF) and their reciprocal depression in the opposite limb leads (I, aVL). Due to the decrease in Na^+/K^+-ATPase protein expression, the resting membrane potential of injured cardiomyocytes shifted toward depolarization. Such induced electrical difference between the injured and intact cardiomyocytes was thought to be responsible for the creation of "currents of injury" and the subsequent ST segment changes.

KEYWORDS: bullfrog heart, inferior wall myocardial infarction, Na^+/K^+-ATPase expression, reciprocal ST segment depression

Inferior wall myocardial infarction accounts for 40–50% of all cases of acute myocardial infarction [1]. Inferior wall myocardial infarction generally has a more favorable prognosis than anterior wall myocardial infarction. However, its serious complications, such as high-degree atrioventricular block and severe hypotension due to right ventricular infarction, are often associated with worse outcomes [1]. To quickly diagnose acute myocardial infarction to improve the patients' outcomes, the electrocardiogram (ECG) analysis is the most useful approach [19]. However, in inferior wall myocardial infarction, the typical ECG changes represented by an elevation of the ST segment cannot always be detected obviously, since the degree of such change is often subtle in ECG limb leads [21]. Besides, the presence of the ST segment elevation alone does not confirm the diagnosis of acute myocardial infarction, because it is also observed in other cardiac disorders, including early repolarization, acute pericarditis, right bundle-branch block and Takotsubo cardiomyopathy [7, 12]. "Reciprocal" ST segment change refers to a ST segment depression in ECG leads opposite to those that detect the ST segment elevation [20], which is frequently observed in acute inferior or anterior myocardial infarction. Since the reciprocal ST segment change is the finding characteristic to acute myocardial infarction, the presence of this change would confirm its diagnosis [3, 24]. In our previous studies, by simply inducing burn injuries on bullfrog hearts or partially exposing them to high-potassium (K^+) or -magnesium (M^{2+}) solutions, we reproduced a ST segment elevation in ECG, which is characteristically observed in human ischemic heart disease [9, 10, 16]. Recently, by inducing burn injuries on the opposite side of the frog heart ventricle, we could additionally reproduce the reciprocal ST segment depression in ECG [13]. Here, by inducing subepicardial burn injuries on the inferior part of frog heart ventricle, we were able to reproduce typical ECG changes mimicking those observed in human inferior wall myocardial infarction. By recording the action potential of cardiomyocytes and using immunohistochemistry, we additionally investigated the Na^+/K^+-ATPase protein expression and its function in burned heart ventricle. This study demonstrated the physiological mechanisms that underly the ECG changes typically observed in inferior wall myocardial infarction.

Adult bullfrogs weighing between 450 and 550 g (*n*=12) were bought from Ohuchi Shōten (Saitama, Japan) and were used in the following experiments. After initial induction of anesthesia with isoflurane (Pfizer Inc., New York, NY, USA), the frogs received intramuscular injection of ethyl carbamate (0.50 g/kg; Wako Pure Chemical Industries, Ltd., Osaka, Japan), a long-acting anesthetic, as we described previously [9–11, 13, 16, 22]. Under profound anesthesia, needle electrodes, which were made of silver wires coated with the layer of silver chloride and soldered to the output pins, were deeply inserted into the upper and lower limbs of the frog (Fig. 1). These electrodes were connected to the ECG amplifier and the electrical signals were detected from the limb leads (leads I,
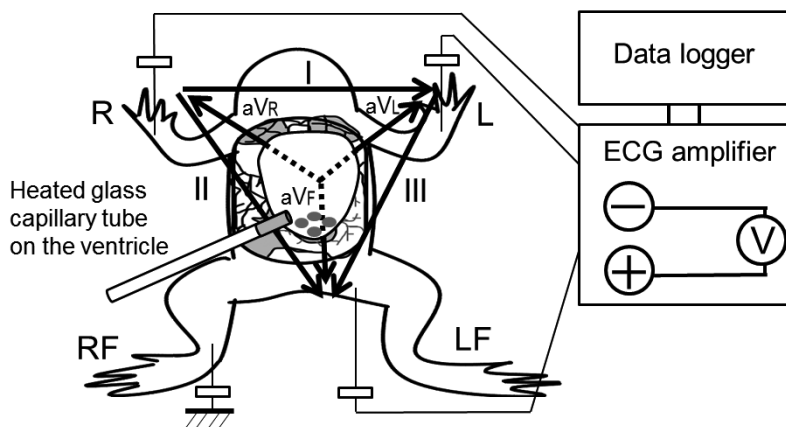
Fig. 1. Detection of electrocardiogram (ECG) signals from the limb leads and induction of inferior wall burn injury in bullfrog heart. Needle electrodes, inserted into the upper and lower limbs of the frog, were connected to the ECG amplifier and the electrical signals were detected by a data logger. In one of the bipolar limb leads, such as in lead I, the left arm (L) electrode served as an exploring electrode (the positive pole) and the right arm (R) electrode as a reference electrode (the negative pole). Likewise, lead II detected the potential difference between the right arm and left leg (LF), while lead III detected the difference between the left arm and left leg. The right leg (RF) electrode served as an electronic reference to improve unwanted noise rejection. In augmented unipolar limb leads, such as in aVR, aVL and aVF, the electrode in the left arm, right arm and left leg respectively served as the positive pole, while the negative pole was composed by averaging the measurements from the other limb electrodes. To induce subepicardial burn injuries on the inferior wall of the myocardium, a heated glass capillary tube was repeatedly placed on the inferior part of the frog heart ventricle.

II, III, aVR, aVL and aVF). In one of the bipolar limb leads, such as in lead I, the left arm electrode served as an exploring electrode (the positive pole) and the right arm electrode as a reference electrode (the negative pole), which detected the potential difference between the right and left arms [4, 15] (Fig. 1). Likewise, lead II detected the potential difference between the right arm and left leg, while lead III detected the difference between the left arm and left leg (Fig. 1). The right leg electrode served as an electronic reference to improve unwanted noise rejection (Fig. 1). In augmented unipolar limb leads, such as in aVR, aVL and aVF, the electrode in the left arm, right arm and left leg respectively served as the positive pole, while the negative pole was composed by averaging the measurements from the other limb electrodes [4, 15] (Fig. 1). Then ECG waveforms obtained from these limb leads were detected and recorded in a data logger (midi LOGGER HV GL2000, GRAPHTEC Corp., Yokohama, Japan). To induce subepicardial injury on the inferior wall of the frog heart ventricle, the frog heart was surgically exposed. Then, as we previously described [9, 13], the tip of a glass capillary tube (1.5 mm in diameter) was heated to more than 600°C in a flame, and was quickly pressed onto the inferior part of the ventricular surface (Fig. 1). By repeating such procedure several times, some overlapping burn injuries were generated in the subepicardial myocardium on the inferior wall of the frog heart (n=5). At the end of the experiments, we euthanized the frogs by the anesthetic overdose of ethyl carbamate. All experimental protocols were approved by the Ethics Review Committee for Animal Experimentation of Miyagi University. Experimental data were analyzed by Microsoft Excel (Microsoft Corp., Redmond, WA, USA) and reported as means ± standard error of the mean. Statistical significance was assessed by Student's t test. A value of $P<0.05$ was considered significant.

In our previous studies, using electrodes directly placed on the ventricular surface of frog hearts (precordial leads), we obtained ECG waveforms that were almost identical to those of humans [9–11, 13, 16, 22]. In the present study, the amplitudes of ECG waveforms detected from the limb leads were much smaller than those detected from the precordial leads (Fig. 2, left). However, these waveforms were also enough to demonstrate a series of distinguishable QRS complexes and the following T waves (Fig. 2, left), between which the ST segments were recorded on the isoelectric lines. Then, immediately after burn injuries were made on the inferior part of the ventricular surface (Fig. 1), the ECG detected from the leads II, III and aVF demonstrated marked elevations of the ST segments (Fig. 2, right). As we previously demonstrated, such changes in the ST segments indicated that myocardial injuries were induced in the frog heart ventricle [9, 13]. Additionally, the pattern of changes in these limb leads mimicked those typically observed in acute inferior myocardial infarction in humans [21]. By contrast, the ECG detected from the leads aVL and I showed obvious depressions of the ST segments from the isoelectric lines (Fig. 2, right). These findings also mimicked the reciprocal ST segment changes frequently observed in human inferior wall myocardial infarction [5, 21]. In general, the presence of reciprocal changes in ECG reflects the extent of myocardial ischemia [8] and supports the diagnosis of acute myocardial infarction [3, 24]. Of note, in cases of inferior myocardial infarction, the presence of such reciprocal ST segment depression in lead aVL clinically indicates the occlusion of the right coronary artery as the culprit lesion [2]. Therefore, the typical ECG findings reproduced in our frog heart model would help to determine the target vessel for revascularization, consequently facilitating the rapid initiation of coronary angioplasty.

For immunohistochemistry, intact frog hearts (n=5) were harvested before burn injuries were induced, which were compared to those harvested immediately after burn injuries were induced (Fig. 1). Cross sections of the hearts were fixed in 4% paraformaldehyde, embedded in paraffin, deparaffinized in xylene, and then 3-µm sections were stained with Masson's trichrome (Fig. 3A). In normal
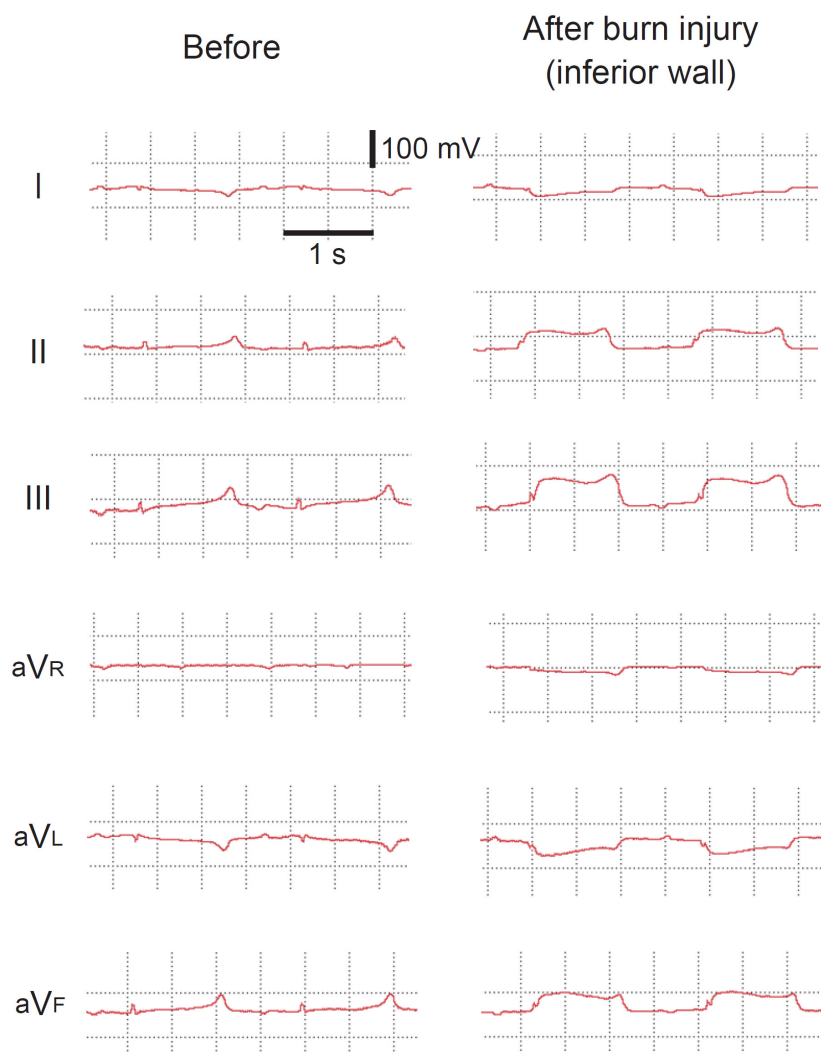
Fig. 2. Changes in electrocardiogram (ECG) before and after burn injuries were induced on the inferior wall. ECG detected from the bipolar limb leads (I, II and III) and unipolar limb leads (aVR, aVL and aVF) before (*left*) and after burn injuries were induced on the inferior part of the ventricle (*right*).

frog hearts, the surface of the ventricle was composed of massive layers of cardiac muscles, which was covered by the thin layers of epicardium (visceral pericardium) (Fig. 3A, top left). After inducing burn injuries, the majority of the cardiac muscles were fibrously degenerated and became atrophic (Fig. 3A, top right). Due to the accumulation of fibrous material, the connective tissue layers within the epicardium became thicker. Na^+/K^+-ATPase is an active pump, which constantly transports sodium (Na^+) ions out of cells but potassium (K^+) ions into the cells [6]. In our recent studies, the functional blockade of this pump activity was deeply associated with the ST segment elevation in ECG [10, 16]. In the present study, the ST segment elevation and its reciprocal depression was similarly induced by myocardial burn injuries (Fig. 2). Therefore, we examined the expressional difference of Na^+/K^+-ATPase before and after burn injuries were made in the frog heart ventricle (Fig. 3A, bottom). Consistent with our previous findings [10, 13, 16], immunohistochemistry demonstrated that Na^+/K^+-ATPase α-subunit protein (1:50; Santa Cruz Biotechnology, Inc., Dallas, TX, USA) almost ubiquitously expressed on the plasma membrane of cardiomyocytes in normal frog heart ventricles (Fig. 3A, bottom left). However, in the fibrously degenerated or atrophic cardiac muscles after the burn injury, the expression of Na^+/K^+-ATPase protein almost totally disappeared (Fig. 3A, bottom right).

Since Na^+/K^+-ATPase helps to maintain the resting membrane potential of cells [6], we examined the action potential of cardiomyocytes after bury injuries were induced (Fig. 3B). To monitor the transmembrane action potential, we employed the suction-electrode method as described previously [9–11, 16, 22]. As shown in Fig. 3Ba, a chloride-coated silver wire, which was inserted into a polyethylene tube (1 mm in diameter), was used as a recording electrode. It was put on the surface of the frog heart ventricle and connected to the data logger. The tip of the tube was filled with the external solution containing 115 mM NaCl, 2 mM KCl, 2 mM $CaCl_2$, 1 mM $MgCl_2$, 5 mM Hepes and 5 mM Na-Hepes (pH 7.4 adjusted with NaOH). A negative pressure was applied to the recording electrode using a syringe connected to the tube, and the cellular membranes were broken under the tube (Fig. 3Ba). This enabled us to detect
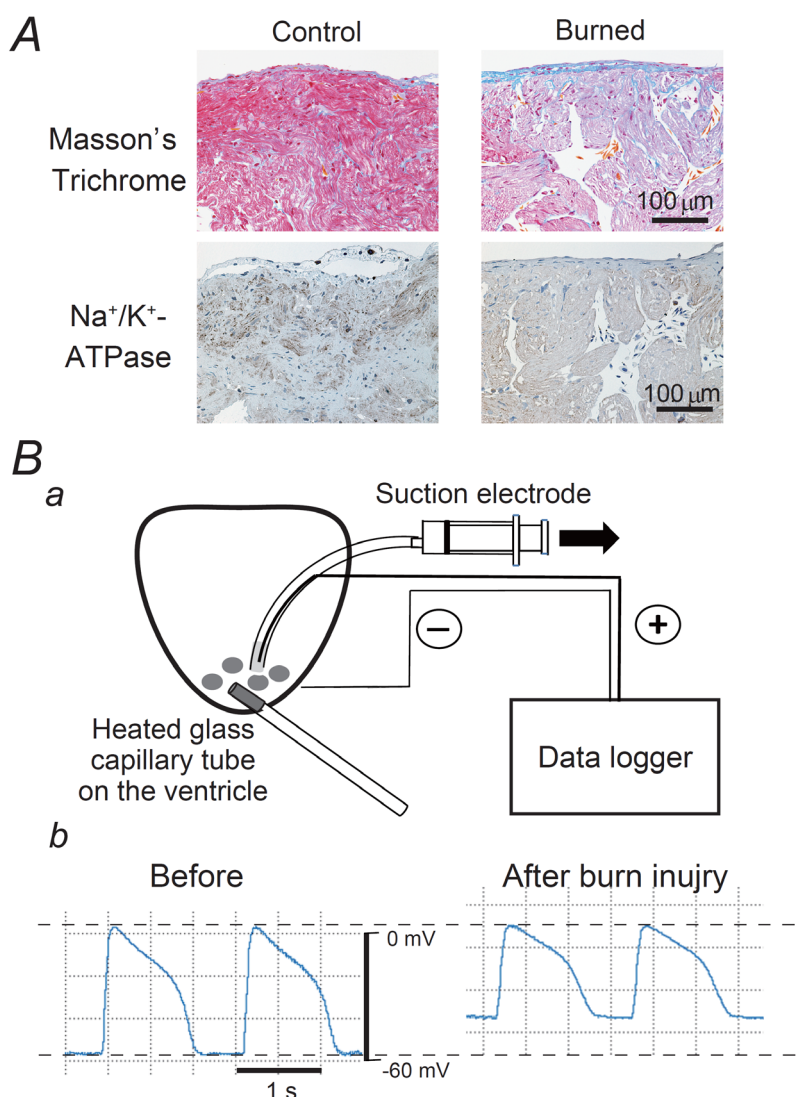
Fig. 3. Na$^+$/K$^+$-ATPase expression and the transmembrane action potential after burn injuries were induced in bullfrog heart. (**A**) *Top*: Masson's trichrome staining in intact ventricular cardiomyocytes (Control) and those after the burn injury (Burned). Magnification × 20. *bottom*: Immunohistochemistry using an antibody for Na$^+$/K$^+$-ATPase α-1 subunit (brown), counterstained with hematoxylin in intact ventricular cardiomyocytes (Control) and those after the burn injury (Burned). Magnification × 20. (**B**) *a*: Suction electrode method was employed to monitor the transmembrane action potential. A negative pressure was applied to the recording electrode, which was placed on the surface of the frog heart ventricle and connected to the data logger. To induce subepicardial burn injury, the heated glass capillary tube was pressed onto the ventricular surface where the transmembrane action potential was recorded. *b*: The action potential of cardiomyocytes was recorded before (*left*) and after burn injuries were induced (*right*).

the compound action potentials from the crowds of cells under the tube [18]. The experiments were performed at room temperature (22–24°C). Before inducing burn injuries, the action potential of cardiomyocytes demonstrated typical waveforms representing the depolarization and repolarization cycles (Fig. 3Bb, left), which were followed by the resting membrane potential in-between. After burn injuries were induced in the same way as we did in Fig. 1, the suction-electrode was directly put on the burned surface of the frog heart ventricle (Fig. 3Ba). The cardiac action potentials obtained from the 5 crowds of burned cells out of 2 bullfrog hearts demonstrated a marked shift of the resting membrane potential to the depolarized side (Fig. 3Bb, right), showing statistical significance (15.2 ± 1.36 mV shift toward depolarization, *n*=5). In the present study, the amplitudes of the action potentials were smaller than those obtained from the conventional method using glass microelectrodes [17]. In our suction-electrode method, as previously demonstrated in frog hearts [23], a tight seal could not be obtained between the cardiac muscles and the polyethylene tube due to the large orifice of the tube.

In our previous studies, the exposure to high- K$^+$ or high- Mg^{2+} solutions functionally blocked the activity of Na$^+$/K$^+$-ATPase in cardiomyocytes, which inhibited the inward transportation of K$^+$ ions [16, 22]. This increased the extracellular K$^+$ concentration, but decreased the intracellular K$^+$ concentration instead. In the present study, the protein expression of Na$^+$/K$^+$-ATPase was almost totally disappeared in fibrously degenerated cardiac muscles after the burn injury (Fig. 3A). Similarly to the "functional" blockade caused
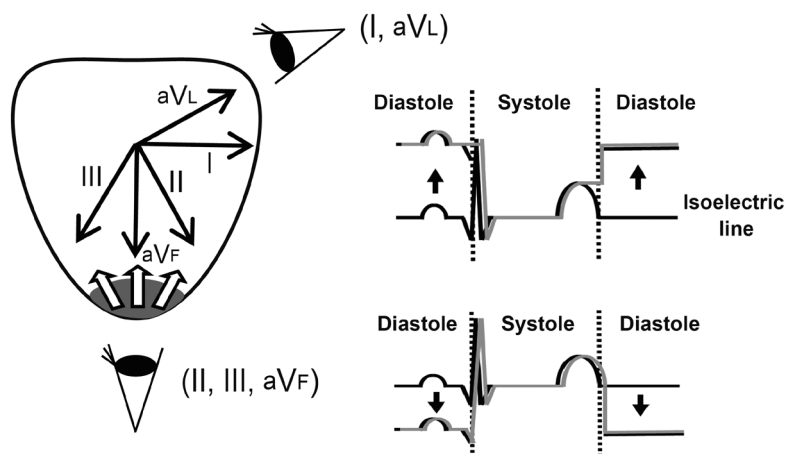
Fig. 4. Mechanisms of reciprocal ST segment changes in inferior wall burn injury model. Leads II, III and aVF are expressed as if they observe (view) the heart from the inferior wall of the ventricle. When myocardial injury was induced on the inferior wall of the ventricular surface, the currents of injury flowed away from the views of the leads II, III and aVF (white arrows). Thus, electrocardiogram (ECG) vector during diastole was negatively deflected from the isoelectric line (arrows), making the ST segment appear elevated during systole (gray waveform). On the other hand, leads aVL and I are expressed as if they observe (view) the heart from the superior part of the ventricle, which is almost opposite to the direction of the lead III. When myocardial injury was induced on the inferior wall of the ventricle, the currents of injury flowed nearly towards the views of the leads aVL and I (white arrows). This caused the ECG vector to be positively deflected during diastole (arrows), making the ST segment appear depressed during systole (gray waveform).

by high K^+ or Mg^{2+} [16, 22], burn injuries caused the "expressional" blockade of the pump activity in cardiomyocytes. As a result, this restrained the extracellular K^+ ions from being transported back into cardiomyocytes, increasing the ratio of the extracellular over the intracellular K^+ concentrations. In the present study, as we previously predicted from our immunohistochemistry results and the Nernst equation [9, 13], the resting membrane potential actually shifted toward depolarization in injured cardiomyocytes (Fig. 3Bb). Such induced electrical difference in the resting membrane potential between the injured and adjacent intact cardiomyocytes would create the "currents of injury" within the myocardium [14]. Since the resting membrane potential shifted toward depolarization in injured cardiomyocytes during diastole of the cardiac cycle (Fig. 3Bb), the currents physically arose from the injured subepicardium and flowed towards the normal ventricular surface during this phase [14].

Among the limb leads, leads II, III and aVF are called "inferior limb leads", since they detect electric heart vectors directing downwards (Fig. 4, left), with the electrode in the left leg serving as the positive pole. In other words, these inferior limb leads could be expressed as if they primarily observe (view) the heart from the inferior wall of the ventricle (Fig. 4, left). When myocardial injury was induced on the inferior wall of the ventricular surface (Fig. 4, left), the currents of injury flowed away from the views of the leads II, III and aVF (white arrows). Because these currents flowed during diastole of the cardiac cycle, the ECG vector during this phase was negatively deflected from the isoelectric line (Fig. 4, right bottom), which alternatively made the ST segment appear elevated during systole (Fig. 4, right bottom). In contrast to the inferior limb leads, leads aVL and I detect electric heart vectors directing the superior part of the ventricle (Fig. 4, left), with the electrode in the left arm serving as the positive pole in both leads. These leads are also expressed as if they primarily observe (view) the heart from the superior part of the ventricle (Fig. 4, left), which is almost opposite to the direction of the lead III. Therefore, when myocardial injury was induced on the inferior wall of the ventricle (Fig. 4, left), the currents of injury flowed nearly towards the views of the leads aVL and I (white arrows). This caused the ECG vector to be positively deflected during diastole (Fig. 4, right top), alternatively making the ST segment appear depressed during systole.

In conclusion, by inducing subepicardial burn injuries on the inferior part of the frog heart ventricle, we could reproduce typical ECG changes mimicking those observed in human inferior wall myocardial infarction. Due to the decrease in Na^+/K^+-ATPase protein expression, the resting membrane potential of injured cardiomyocytes elevated. Such induced electrical difference between the injured and intact cardiomyocytes was thought to be responsible for the creation of "currents of injury" and the subsequent ST segment changes typically observed in inferior wall myocardial infarction.

REFERENCES

1. Berger PB, Ryan TJ. 1990. Inferior myocardial infarction. High-risk subgroups. *Circulation* **81**: 401–411. [Medline] [CrossRef]
2. Birnbaum Y, Drew BJ. 2003. The electrocardiogram in ST elevation acute myocardial infarction: correlation with coronary anatomy and prognosis.

Postgrad Med J **79**: 490–504. [Medline] [CrossRef]

3. Brady WJ, Perron AD, Syverud SA, Beagle C, Riviello RJ, Ghaemmaghami CA, Ullman EA, Erling B, Ripley A, Holstege C. 2002. Reciprocal ST segment depression: impact on the electrocardiographic diagnosis of ST segment elevation acute myocardial infarction. *Am J Emerg Med* **20**: 35–38. [Medline] [CrossRef]

4. Dower GE, Nazzal SB, Pahlm O, Haistey WK Jr, Marriott HL, Bullington RH, Bullington D. 1990. Limb leads of the electrocardiogram: sequencing revisited. *Clin Cardiol* **13**: 346–348. [Medline] [CrossRef]

5. Gibelin P, Gilles B, Baudouy M, Guarino L, Morand P. 1986. Reciprocal ST segment changes in acute inferior myocardial infarction: clinical, haemodynamic and angiographic implications. *Eur Heart J* **7**: 133–139. [Medline] [CrossRef]

6. Glitsch HG. 2001. Electrophysiology of the sodium-potassium-ATPase in cardiac cells. *Physiol Rev* **81**: 1791–1826. [Medline] [CrossRef]

7. Hanna EB, Glancy DL. 2015. ST-segment elevation: differential diagnosis, caveats. *Cleve Clin J Med* **82**: 373–384. [Medline] [CrossRef]

8. Hwang JW, Yang JH, Song YB, Park TK, Lee JM, Kim JH, Jang WJ, Choi SH, Hahn JY, Choi JH, Ahn J, Carriere K, Lee SH, Gwon HC. 2019. Clinical significance of reciprocal ST-segment changes in patients with STEMI: a cardiac magnetic resonance imaging study. *Rev Esp Cardiol (Engl Ed)* **72**: 120–129. [Medline] [CrossRef]

9. Kazama I. 2016. Burn-induced subepicardial injury in frog heart: a simple model mimicking ST segment changes in ischemic heart disease. *J Vet Med Sci* **78**: 313–316. [Medline] [CrossRef]

10. Kazama I. 2021. High-magnesium exposure to bullfrog heart causes ST segment elevation. *J Vet Med Sci* **83**: 675–679. [Medline] [CrossRef]

11. Kazama I. 2017. High-calcium exposure to frog heart: a simple model representing hypercalcemia-induced ECG abnormalities. *J Vet Med Sci* **79**: 71–75. [Medline] [CrossRef]

12. Kazama I, Nakajima T. 2019. Apparent ST elevation in right bundle branch block pseudo-mimicking myocardial infarction. *SAGE Open Med Case Rep* **7**: 2050313X19827748. [Medline] [CrossRef]

13. Kazama I, Takamura K, Yamada Y, Sugisaki Y, Suzuki M. 2020. Reciprocal ST segment changes reproduced in burn-induced subepicardial injury model in bullfrog heart. *J Vet Med Sci* **82**: 143–147. [Medline] [CrossRef]

14. Kléber AG. 2000. ST-segment elevation in the electrocardiogram: a sign of myocardial ischemia. *Cardiovasc Res* **45**: 111–118. [Medline] [CrossRef]

15. Kligfield P, Gettes LS, Bailey JJ, Childers R, Deal BJ, Hancock EW, van Herpen G, Kors JA, Macfarlane P, Mirvis DM, Pahlm O, Rautaharju P, Wagner GS, Josephson M, Mason JW, Okin P, Surawicz B, Wellens H, American Heart Association Electrocardiography and Arrhythmias Committee, Council on Clinical Cardiology, American College of Cardiology Foundation Heart Rhythm Society. 2007. Recommendations for the standardization and interpretation of the electrocardiogram: part I: The electrocardiogram and its technology: a scientific statement from the American Heart Association Electrocardiography and Arrhythmias Committee, Council on Clinical Cardiology; the American College of Cardiology Foundation; and the Heart Rhythm Society: endorsed by the International Society for Computerized Electrocardiology. *Circulation* **115**: 1306–1324. [Medline] [CrossRef]

16. Kon N, Abe N, Miyazaki M, Mushiake H, Kazama I. 2018. Partial exposure of frog heart to high-potassium solution: an easily reproducible model mimicking ST segment changes. *J Vet Med Sci* **80**: 578–582. [Medline] [CrossRef]

17. Niedergerke R, Orkand RK. 1966. The dual effect of calcium on the action potential of the frog's heart. *J Physiol* **184**: 291–311. [Medline] [CrossRef]

18. Stys PK, Ransom BR, Waxman SG. 1991. Compound action potential of nerve recorded by suction electrode: a theoretical and experimental analysis. *Brain Res* **546**: 18–32. [Medline] [CrossRef]

19. Thygesen K, Alpert JS, Jaffe AS, Simoons ML, Chaitman BR, White HD, Katus HA, Lindahl B, Morrow DA, Clemmensen PM, Johanson P, Hod H, Underwood R, Bax JJ, Bonow RO, Pinto F, Gibbons RJ, Fox KA, Atar D, Newby LK, Galvani M, Hamm CW, Uretsky BF, Steg PG, Wijns W, Bassand JP, Menasché P, Ravkilde J, Ohman EM, Antman EM, Wallentin LC, Armstrong PW, Simoons ML, Januzzi JL, Nieminen MS, Gheorghiade M, Filippatos G, Luepker RV, Fortmann SP, Rosamond WD, Levy D, Wood D, Smith SC, Hu D, Lopez-Sendon JL, Robertson RM, Weaver D, Tendera M, Bove AA, Parkhomenko AN, Vasilieva EJ, Mendis S, Joint ESC/ACCF/AHA/WHF Task Force for the Universal Definition of Myocardial Infarction. 2012. Third universal definition of myocardial infarction. *Circulation* **126**: 2020–2035. [Medline] [CrossRef]

20. Vaidya GN, Antoine S, Imam SH, Kozman H, Smulyan H, Villarreal D. 2018. Reciprocal ST-segment changes in myocardial infarction: ischemia at distance versus mirror reflection of ST-elevation. *Am J Med Sci* **355**: 162–167. [Medline] [CrossRef]

21. Whalen D, Dunne C, Dubrowski A, Mohamed L, Parsons MH. 2019. Diagnosis and management of an inferior ST-elevation myocardial infarction: a simulation scenario. *Cureus* **11**: e3995. [Medline]

22. Yeoh RN, Akiyama Y, Senzaki M, Kazama I. 2021. Insulin accelerates recovery from QRS complex widening in a frog heart model of hyperkalemia. *J Vet Med Sci* **83**: 1855–1859. [Medline] [CrossRef]

23. Yoshida S. 2001. Simple techniques suitable for student use to record action potentials from the frog heart. *Adv Physiol Educ* **25**: 176–186. [Medline] [CrossRef]

24. Yousif H, Lo E, Taha T, Stockins B, Oakley CM. 1989. The diagnostic significance of reciprocal ST segment depression in acute myocardial infarction. *Q J Med* **72**: 849–855. [Medline]